

# Star formation history, double degenerates and type Ia supernovae in the thin disc

Shenghua Yu\* and C. Simon Jeffery †

Armagh Observatory, College Hill, Armagh BT61 9DG, N. Ireland

Accepted . Received ;

## ABSTRACT

We investigate the relation between the star formation history and the evolution of the double-degenerate (DD) population in the thin disc of the Galaxy, which we assume to have formed 10 Gyr before the present. We introduce the use of star-formation contribution functions as a device for evaluating the birth rates, total number and merger rates of DDs. These contribution functions help to demonstrate the relation between star-formation history and the current DD population and, in particular, show how the numbers of different types of DD are sensitive to different epochs of star formation.

Analysis of the contribution functions given by a quasi-exponentially decline in the star-formation rate shows that star formation from 0 to 8 Gyr after thin-disc formation dominates the present rates and total numbers of He+He DDs and CO+He DDs. Similarly, the current numbers of CO+CO and ONeMg+X DDs come mainly from early star formation ( $< 6$  Gyr), although star formation from 4 to 8 Gyr continued to contribute more CO+CO than He+He DDs. The present birth-rates for CO+CO and ONeMg+X DDs are strongly governed by recent star formation (*i.e.* 8 – 9.95 Gyr). Star formation from  $< 7.5$  Gyr does *not* contribute to the present birth rates of CO+CO and ONeMg+X DDs, but it has a distinct contribution to their merger rates.

We have compared the impact of different star-formation models on the rates and numbers of DDs and on the rates of type Ia (SNIa) and core-collapse supernovae (ccSN). In addition to a quasi-exponential decline model, we considered an instantaneous (or initial starburst) model, a constant-rate model, and an enhanced-rate model. All were normalised to produce the present observed star density in the local thin disc. The evolution of the rates and numbers of both DDs and SNIa are different in all four models, but are most markedly different in the instantaneous star-formation model, which produces a much higher rate than the other three models in the past, primarily as a consequence of the normalisation.

Predictions of the current SNIa rate range from  $\approx 2$  to  $5 \times 10^{-4} \text{ yr}^{-1}$  in the four models, and are slightly below the observed rate because we only consider the DD merger channel. The predicted ccSN rate ranges from 1.5 to 3 century $^{-1}$ , and is consistent with observations.

**Key words:** stars: white dwarfs – stars: evolution – stars: binaries: close – supernovae: general – Galaxy: evolution – Galaxy: structure

## 1 INTRODUCTION

We know little about the star formation (SF) history of the Milky Way disc. Of the few ways available to explore the SF history, studying the stellar age distribution by the observation of a sample of different types of stars and comparing observed and synthetic colour-magnitude diagrams would be the most favored approach. The simplest view of the SF history would be a single star burst taking place at the formation of the disc. Substantial evidence, how-

ever, shows the disc has experienced a more complicated history, including repeated star bursts, an exponential declining SF or extended periods of enhanced SF (Majewski 1993; Rocha-Pinto et al. 2000) or some combination of all of these.

The present SF rate is better understood. Smith et al. (1978) concludes the SF rate in the Galaxy is perhaps  $5 M_{\odot} \text{ yr}^{-1}$ , of which 74% take place in spiral arms, 13% in the interarm region, and 13% in the galactic center. Observations of Lyman continuum photons from O stars in giant H II regions give the SF rate in the disc to be  $4.35 M_{\odot} \text{ yr}^{-1}$ . A SF rate  $\approx 3.6 M_{\odot} \text{ yr}^{-1}$  was suggested by McKee (1989) from an analysis of thermal radio emission in HII regions around massive stars. The measurement of the mass of  $^{26}\text{Al}$  in

\* E-mail: syu@arm.ac.uk (SY)

† E-mail: csj@arm.ac.uk (CSJ)

the Galaxy implies a SF rate  $\approx 4 M_{\odot} \text{yr}^{-1}$  (Diehl et al. 2006). The derivation of the SF rate is strongly associated with the initial mass function (namely the distribution of the mass of the new-born stars) and the birth rate of core collapse supernovae (type Ib/c and type II).

Double degenerates (DDs) are a type of exotic binary consisting of two white dwarfs. As the evolved remnants of stars, the formation of close DDs requires their progenitors to have undergone a mass transfer stage, either common envelope or stable Roche lobe overflow phase. Ultra-compact DDs are especially interesting since not only can they be observed as active sources of electromagnetic radiation, *e.g.* AM Canum Venaticorum stars, (Cropper et al. 1998; Ramsay et al. 2005; Nelemans et al. 2004), but also the final products of DD evolution may include type Ia supernovae (Yungelson & Livio 2000)). Theoretical results (Evans et al. 1987; Nelemans et al. 2001; Ruiter et al. 2010; Yu & Jeffery 2010) suggest that close DDs should also be significant sources of gravitational wave radiation, and be detectable by the space gravitational wave (GW) detector LISA (Laser Interferometer Space Antennae).

The census of DDs therefore is important because they allow us to test the endpoints of stellar evolution. We need to know the present-day numbers, birth rates, merger rates and galactic distribution of DDs, and also the distribution of their properties (*i.e.* mass, orbital separation, chemical abundance and age). To interpret these, we need to investigate how the history of star formation in the Galaxy affects the DD population. We can achieve this using a population synthesis approach.

In this paper, we study the correlation of the SF history and the evolution of DD population. It may help interpret the distribution of the physical properties of DDs as a function of the SF history. In §2, we describe the approach to simulate a population of the DDs in the thin disc and discuss the details of how a quasi-exponential declining SF rate influences the birth rate, merger rate and total number of DDs. In §3, we show the distributions of some important physical parameters of the DDs from different epochs of SF. In §4, we compare the impact of different SF models on the rates and numbers of DDs. We discuss the results for supernovae rates in different SF models in §5. Some points are discussed in §6 and conclusions are drawn in §7.

## 2 POPULATION SYNTHESIS OF THIN DISC DDS IN THE MONTE CARLO APPROACH

In this section, we describe the population synthesis method to obtain a sample of DDs comparable with current observations, and the structure of the thin disc in which the DD population is distributed. The individual stellar-evolution tracks were computed using the method described by Hurley et al. (2000, 2002). Population synthesis was carried out using the method described by Yu & Jeffery (2010) in an initial study of the present Galactic DD population.

### 2.1 The star-formation contribution function

We define a time representing the age of the thin disc to be  $t$ , such that the disc formed at  $t = 0$ , and the current age of the thin disc is  $t_{\text{disc}}$ . During the evolution of the thin disc, we assume that star formation takes place over an interval  $t = t_{\text{sf}}$  ( $0 \leq t_{\text{sf}} \leq t_{\text{disc}}$ ) to  $t = t_{\text{sf}} + \delta t_{\text{sf}}$ . We simulate the evolution of all binaries formed during this interval by computing a sample (denoted by  $*$ ) of  $k$  primordial MS+MS (MS: main sequence) binaries with a total mass

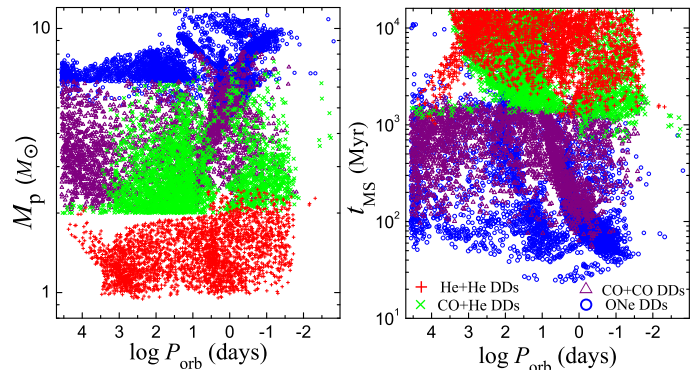


**Figure 1.** The orbital periods ( $\log P_{\text{orb}}/\text{day}$ ) of the DDs against the primary masses ( $M_p$ , left panel) in the MS+MS binary progenitors and the time ( $t_{\text{MS}}$ , right panel) which is from a primordial MS+MS binary to when its descendant DD was just born.

$M_*^1$ . This gives a mean *sample* SF rate  $S_* = M_*/\delta t_{\text{sf}}$ .  $\delta t_{\text{sf}}$  is assumed to be small; thus all primordial MS+MS binaries formed during this interval evolve as though they formed at time  $t_{\text{sf}}$ . The binary-star evolution tracks are computed as a function of  $t$  over the interval  $\log(t/\text{yr}) = 7.4 - 10.13$  with  $\delta \log t = 0.00867$ .

We then compute the contribution of star formation during the interval  $\delta t_{\text{sf}}$  to the birth-rate, total number and merger-rate of DDs at time  $t = t_{\text{disc}}$  (the present epoch). This interval is denoted by the quantity  $\Delta = t_{\text{disc}} - t_{\text{sf}}$ .

For a given age of the thin disc  $t_{\text{disc}}$ , star formation in the thin disc runs from  $t_{\text{sf}} = 0$  to  $t_{\text{disc}}$ . For convenience, we use  $\delta \log t_{\text{sf}} = \delta \log t_{\text{disc}}$ .

Two additional time variables are used to establish the stage of evolution of DDs in the sample.  $t_{\text{MS}}$  represents the lifetime from birth of an individual binary system to the formation of a DD.  $t_{\text{DD}}$  represents the lifetime from formation of a DD to its merger<sup>2</sup>.

The birth-rate contribution is established by counting the number of DDs which form during the interval  $t_{\text{disc}}$  to  $t_{\text{disc}} + \delta t_{\text{disc}}$ . These are stars for which

$$t_{\text{disc}} \leq t_{\text{sf}} + t_{\text{MS}} < t_{\text{disc}} + \delta t_{\text{disc}}. \quad (1)$$

Normalising by the mean sample SF rate  $S_*$  gives the fractional number  $\delta n_{*,\text{new}}(\Delta)$  of DDs born per unit mass of star's formed between  $t = t_{\text{sf}}$  and  $t_{\text{sf}} + \delta t_{\text{sf}}$ .

The merger-rate contribution is established in an analogous way. Counting stars for which

$$t_{\text{disc}} \leq t_{\text{sf}} + t_{\text{MS}} + t_{\text{DD}} < t_{\text{disc}} + \delta t_{\text{disc}}, \quad (2)$$

gives the fraction  $\delta n_{*,\text{mer}}(\Delta)$ .

The total-number contribution  $\delta n_{*,\text{dd}}(\Delta)$  represents the fractional number of DDs in the sample which exist at time  $t_{\text{disc}}$ . These stars are identified by

$$t_{\text{sf}} + t_{\text{MS}} < t_{\text{disc}} \leq t_{\text{sf}} + t_{\text{MS}} + t_{\text{DD}}. \quad (3)$$

<sup>1</sup> We make the assumption that the global properties of the MS+MS binary population from each star formation episode are the same; *i.e.* each sample adopts the same initial parameter distribution.

<sup>2</sup> We have assumed the angular momentum evolution of a DD to be governed only by gravitational wave radiation and mass transfer (Yu & Jeffery 2010), although tidal interaction and magnetic braking may play an important role (Marsh et al. 2004; Gokhale et al. 2007; Farmer & Roelofs 2010).

**Table 1.** The variables in the population synthesis simulation and their relationship.

|   |  |
|---|--|
| time  |  |
| $t_{\text{disc}}$   | the age of the thin disc   |
| $t_{\text{sf}}$   | the time of star formation (SF)<br>( $0 \leq t_{\text{sf}} \leq t_{\text{disc}}$ )                         |
| $\Delta = t_{\text{disc}} - t_{\text{sf}}$  | delay time<br>from SF to the disc age  |
| <hr/>   |  |
| Thin disc   |  |
| $n(t_{\text{disc}})$  | total number   |
| $\dot{n}(t_{\text{disc}})$  | number rate  |
| $\dot{C}(\Delta)$   | contribution function to $n$   |
| $\ddot{C}(\Delta)$  | rate contribution function to $\dot{n}$  |
| $S(t_{\text{sf}})$  | SF rate  |
| <hr/>   |  |
| Sample <sup>†</sup>   |  |
| $\delta n_*(\Delta)$  | number at $t_{\text{disc}}$<br>from SF at $t_{\text{sf}} \rightarrow t_{\text{sf}} + \delta t_{\text{sf}}$ |
| $\dot{C}_*(\Delta)$   | contribution function  |
| $\ddot{C}_*(\Delta)$  | rate contribution function   |
| $S_*(t_{\text{sf}})$  | mean SF rate in the sample   |
| <sup>†</sup> All the values normalized by $S_*(t_{\text{sf}})$ .  |  |
| <hr/>   |  |
| Identities  |  |
| $\dot{C}_*(\Delta) = \partial n_*(\Delta) / \partial t_{\text{sf}}$<br>$\approx \delta n_*(\Delta) / \delta t_{\text{sf}}$    |  |
| $\ddot{C}_*(\Delta) = \frac{\partial^2 n_*(\Delta)}{\partial t_{\text{sf}}^2 \partial t_{\text{disc}}}$                       |  |
| $\dot{C}(\Delta) = \dot{C}_*(\Delta) \cdot S(t_{\text{sf}})$  |  |
| $\ddot{C}(\Delta) = \ddot{C}_*(\Delta) \cdot S(t_{\text{sf}})$  |  |
| $n(t_{\text{disc}}) = \int_0^{t_{\text{disc}}} \dot{C}(t_{\text{disc}} - t) dt$<br>$= \int_0^{t_{\text{disc}}} \dot{n}(t) dt$ |  |
| $\dot{n}(t_{\text{disc}}) = \int_0^{t_{\text{disc}}} \ddot{C}(t_{\text{disc}} - t) dt$  |  |

These three quantities, let us call them star-formation number contribution functions  $\delta n_*$ , comprising  $\delta n_{*,\text{new}}$ ,  $\delta n_{*,\text{dd}}$  and  $\delta n_{*,\text{mer}}$ , may then be combined with a model for the star formation history of the thin disc  $S(t)$  to establish the *total* current birth-rate, merger rate and number of DDs.

From above, we have  $\delta n_*(\Delta)$  to be the SF contribution at time  $t_{\text{sf}}$  to the number per unit SF rate at time  $t_{\text{sf}}$ , integrated over an interval  $\delta t_{\text{sf}}$ . Hence  $\dot{C}_* = \partial n_*/\partial t_{\text{sf}} \approx \delta n_*/\delta t_{\text{sf}}$  is the sample contribution function per unit SF rate per unit time at time  $t_{\text{sf}}$ .

To obtain total numbers in a real thin disc, we must multiply by the thin-disc SF rate to obtain the total contribution rates:

$$\dot{C} = \dot{C}_* \cdot S(t_{\text{sf}}) \approx \frac{\delta n_*}{\delta t_{\text{sf}}} \cdot S(t_{\text{sf}}). \quad (4)$$

$\dot{C}$  also reflects the distribution of age of the DDs. For example, if the thin-disc SF rate is  $S(t)$ , star formation at  $t_{\text{sf}} = 0$  will contribute  $\delta n_*(t_{\text{disc}})/\delta t_{\text{sf}} \cdot S(0)$  DDs with age  $t_{\text{disc}}$ ; star formation at  $t_{\text{sf}} = 1$  Gyr will contribute  $\delta n_{\text{ast}}(t_{\text{disc}} - 1)/\delta t_{\text{sf}} \cdot S(1)$  DDs with age  $t_{\text{disc}} - 1$  Gyr, and so on.

Since we know from Eq. 4 that star formation at time  $t_{\text{sf}}$  contributes  $\dot{C}(t_{\text{disc}} - t_{\text{sf}})$  DDs at thin disc age  $t_{\text{disc}}$ , we define a rate contribution function

$$\ddot{C} = \partial \dot{C} / \partial t_{\text{disc}} \quad (5)$$

to be the contribution from star formation at  $t_{\text{sf}}$  to the number rate

at time  $t_{\text{disc}}$ . The integral of the rate contribution function tells us the birth rate and the merger rate of DDs.

## 2.2 Birth rate, merger rate and total number of DDs

We define  $n(t)$  to be the total number of DDs at thin disc age  $t$ , where  $n$  may represent new-born  $n_{\text{new}}$ , merged  $n_{\text{mer}}$  or existing  $n_{\text{dd}}$  DDs. Star formation from  $t_{\text{sf}}$  to  $t_{\text{sf}} + \delta t_{\text{sf}}$  will generate  $\dot{C} \cdot \delta t_{\text{sf}}$  DDs with age  $t_{\text{disc}} - t_{\text{sf}}$ . Hence, the overall number of new-born, alive or merged DDs at  $t = t_{\text{disc}}$  is

$$\begin{aligned} n(t_{\text{disc}}) &= \int_0^{t_{\text{disc}}} \dot{C}(t_{\text{disc}} - t_{\text{sf}}) dt_{\text{sf}} \\ &\approx \sum_{t_{\text{sf}}=0}^{t_{\text{disc}}} \delta n_*(t_{\text{disc}} - t_{\text{sf}}) \cdot S(t_{\text{sf}}) \\ &\approx \sum_{t_{\text{sf}}=0}^{t_{\text{disc}}} \dot{C} \cdot \delta t_{\text{sf}}. \end{aligned} \quad (6)$$

Then we are able to calculate the number rate  $\dot{n}(t_{\text{disc}})$  of DDs from the contribution function  $\ddot{C}$

$$\begin{aligned} \dot{n}(t_{\text{disc}}) &= \int_0^{t_{\text{disc}}} \ddot{C}(t_{\text{disc}} - t_{\text{sf}}) dt_{\text{sf}} \\ &\approx \sum_{t_{\text{sf}}=0}^{t_{\text{disc}}} \frac{\delta n_*(t_{\text{disc}} - t_{\text{sf}})}{\delta t_{\text{sf}}} \cdot S(t_{\text{sf}}) \\ &\approx \sum_{t_{\text{sf}}=0}^{t_{\text{disc}}} \ddot{C} \cdot \delta t_{\text{sf}}, \end{aligned} \quad (7)$$

where  $\dot{n}$  represents the birth rate  $\nu$  or merger rate  $\zeta$ . We will give the details of these functions in the present simulation in §2.4.

Furthermore, since we know the overall rate of change in the number DDs  $\nu(t) - \zeta(t)$ , we can also calculate the total number of DDs in the thin disc at time  $t_{\text{disc}}$  ( $n_{\text{dd}}(t_{\text{disc}})$ ) by the integral

$$\begin{aligned} n_{\text{dd}}(t_{\text{disc}}) &= \int_0^{t_{\text{disc}}} [\nu(t) - \zeta(t)] dt \\ &\approx \sum_{t=0}^{t_{\text{disc}}} [\nu(t) - \zeta(t)] \cdot \delta t. \end{aligned} \quad (8)$$

Consequently, we have two different methods to compute the current number of DDs in the thin disc. Eq. 6 represents the sum of contributions from each individual SF epoch to the total number by counting which DDs exist at the current epoch. Eq. 8 represents the integral of the birth-rate minus the merger-rate, or nett birth rate, over the entire SF history of the galaxy. The two methods should give the same result but, due to the limited grid in  $t_{\text{sf}}$ , the evaluation of the sum in Eq. 6 gives slightly higher numbers than Eq. 8. In the present simulation with quasi-exponential SF rate, the differences are 1.57%, 0.98%, 0.51%, and 0.46% for He+He, CO+He, CO+CO, and ONeMg+X DDs, respectively.

We list the time variables, numbers (rates), contribution functions and their relation in the thin disc and our simulation in Table 1.

## 2.3 Input to the Monte-Carlo simulation

The SF rate is assumed to be given by the quasi-exponential function

$$S(t_{\text{sf}}) = 7.92e^{-(t_{\text{sf}})/\tau} + 0.09(t_{\text{sf}}) \text{ M}_{\odot}\text{yr}^{-1} \quad (9)$$

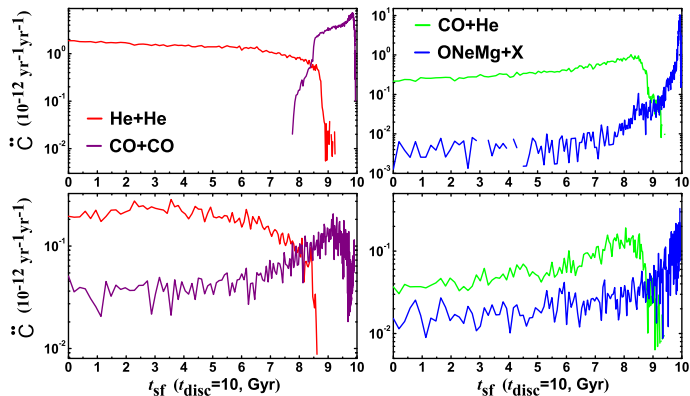


**Figure 2.** The variation of the contribution of star formation  $t_{\text{sf}}$  to the present birth rate and merger rate of DDs,  $\dot{C}$ , in the quasi-exponential star formation rate model. In this figure, top panels represent the contribution to the present birth rate, and bottom panels represent the contribution to the merger rate. See §2.4 for the details.

where  $\tau = 9$  Gyr (Yu & Jeffery 2010), which produces  $\approx 3.5 M_{\odot} \text{yr}^{-1}$  at the current epoch. This is consistent with Diehl et al. (2006).

The contribution function for each starting epoch ( $t_{\text{sf}}$ ) is obtained from a sample of primordial binaries. Each binary is defined by at least five initial parameters: primary mass  $M_{\text{p}}$ , mass-ratio  $q$ , orbital separation  $a$ , eccentricity  $e$  and metallicity  $Z$ . Primary masses  $M_{\text{p}}$  are distributed assuming a power law (Kroupa et al. 1993) for the initial mass function (IMF). This is constrained by the observation of the local luminosity function and stellar density of Wielen et al. (1983) and Popper (1980). A flat distribution is adopted for mass-ratio ( $0 < q < 1$ ) and eccentricity ( $0 < e < 1$ ), since these are not well constrained by observation. The distribution of orbital separation  $a$  is assumed to be constant in logarithm for wide binaries and falls off smoothly at close separations (Han 1998). We have assumed  $Z = 0.02$  throughout. All other input parameters are as given by Yu & Jeffery (2010).

The present population synthesis simulation started with a sample of  $10^7$  primordial MS+MS binaries, with total mass  $\approx 1.05 \times 10^7 M_{\odot}$ , yielding a sample total of  $4.93 \times 10^4$  DDs over all orbital periods of less than 100 yr during a sampling period of 15 Gyr.

In order to evaluate the computation of our DD sample, Fig. 1 shows (left) the orbital periods ( $\log P_{\text{orb}}/\text{day}$ ) of each new-born DD against primary mass ( $M_{\text{p}}$ ) in the progenitors and (right) the time  $t_{\text{MS}}$  from binary-star formation to the birth of its descendant DD. We define DDs in this sample as unevolved DDs. This figure shows the relation of new-born DDs and their progenitors.

## 2.4 The contribution functions in the present simulation

In this section, we investigate how the present number of DDs and the number of new-born DDs depends on the star formation history of the thin disc by examining the contribution functions. We take the current age of the thin disc to be 10 Gyr. Star formation time  $t_{\text{sf}}$  runs from 0 to 10 Gyr. Figures 2 and 3 illustrate the variation of  $\dot{C}$  (rate contributions to the present birth and merger rates) and  $\dot{C}$  (number contributions to the present numbers and total merged numbers) with  $t_{\text{sf}}$ . Equivalently, the figures show us the age distribution of present new born, alive and merged DDs. Since the age of

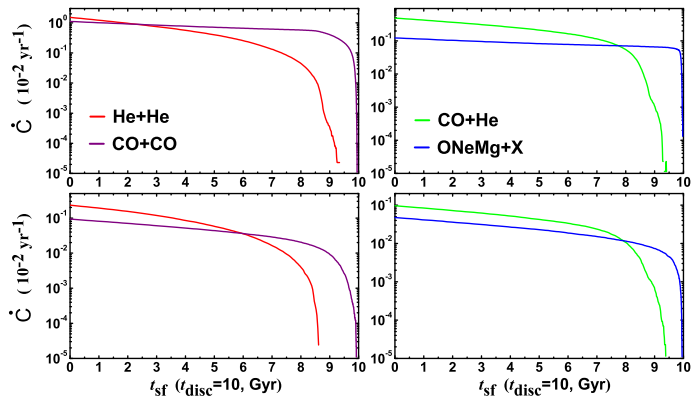


**Figure 3.** Same as Fig. 2 but for the contribution of star formation  $t_{\text{sf}}$  to the present number (top panels) and the total merged number (bottom panels) of DDs,  $\dot{C}$ . See §2.4 for the details.

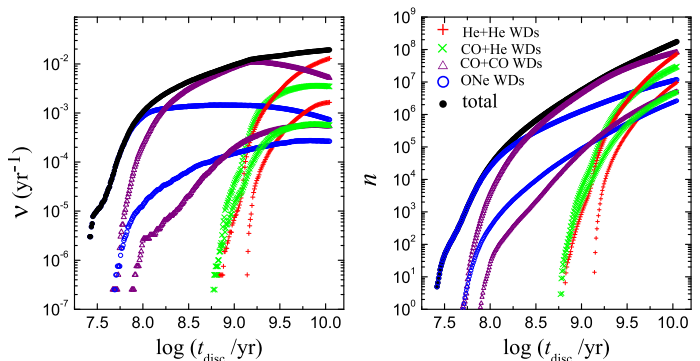


**Figure 4.** Birth rates  $\nu(t)$  (left panel) and merger rates  $\zeta(t)$  (left panel) and numbers  $n(t)$  (right panel) of different types of DD by integral of the corresponding birth and merger rates versus the age of the thin disc  $t_{\text{disc}}$ .  $\nu(t)$  and  $\zeta(t)$  for each type of DD is shown in the same colour, but  $\zeta(t) < \nu(t)$ . Black points are for the nett total birth rate ( $\nu(t) - \zeta(t)$ ) and the total existing number of the DDs.

a DD is defined as  $t_{\text{disc}} - t_{\text{sf}}$  (§2.3), the age distribution is obtained by transforming the x-scale to  $t_{\text{disc}} - t_{\text{sf}}$ .

The top panels in Fig. 2 indicates that the present new-born He+He and CO+He DDs come mainly from early star formation  $t_{\text{sf}} < 8$  Gyr. This is not the case for CO+CO and ONeMg+X DDs. The top panels in Fig. 2 also show that the present new-born CO+CO and ONeMg+X come almost entirely from recent star formation;  $8 < t_{\text{sf}} < 10$  Gyr.

This remarkable discrepancy is basically a result of  $t_{\text{MS}}$ . Figure 1 (right panel) illustrates that a massive MS+MS binary generally takes less than a few Myr and 1 Gyr to form ONeMg+X and CO+CO DDs respectively, leading to their formation much more quickly than He+He and CO+He DDs. This also results in the birth rates of ONeMg+X and CO+CO increasing dramatically at an early stage of disc evolution. Only after some time do CO+He and He+He DDs emerge and do their birth rates grow to reach the present values shown in the left panel of Fig. 4. Due to the quasi-exponential SF rate, the birth rates of ONeMg+X and CO+CO DDs start to decline after reaching a peak value. The long  $t_{\text{MS}}$  for single He white dwarfs also results in a small contribution of star formation from 0–7.5 Gyr to the number of new-born ONeMg+He

DDs at the present. During the same period, there are no new-born CO+CO DDs.

Figure 3 shows that the *contribution* of star formation to the present numbers (top panels) and total merged numbers (bottom panels) of all types of DDs decreases monotonically as a function of  $t_{\text{sf}}$ . This is because most DDs from all epochs survive to the present time due to their wide orbital separations. The number of He+He DDs from each epoch decreases with  $t_{\text{sf}}$  more sharply than for CO+CO DDs, although early star formation provides more He+He DDs than CO+CO DDs. A similar situation arises for CO+He and ONeMg+He DDs. This result is consistent with stellar evolution and the assumed SF rate.

The significance of computing the present number of DDs using Eq. 6, which represents the sum of DDs arising from different star-formation epochs, is that it demonstrates the link between the SF history of the galaxy (or, at least, the thin disc in the present investigation) and the distribution of the properties of present-day DDs, which can be deduced from, for example, their gravitational wave signal.

Figure 4 shows the variation of  $\nu$ ,  $\zeta$  and  $n_{\text{dd}}$  (Eq. 6) of different types of DD with age  $t_{\text{disc}}$ . The individual properties of the current  $n_{\text{dd}}$  DDs will be used to calculate the gravitational wave signal (Yu & Jeffery 2011).

## 2.5 The structure of the thin disc and the local density of DDs

The use of a realistic disc model is important in order to describe the distance distribution of white dwarf binary systems from the Sun. Sackett (1997) proposed a double exponential distribution. Phleps et al. (2000) derived three functions for the star density distribution in their model of a thin disc plus thick disc (exponential + exponential, hyperbolic secant + exponential, and squared hyperbolic secant + exponential, respectively) from fits to deep star counts carried out in the Calar Alto Deep Imaging Survey.

We here model the thin disc in the Galaxy using a squared hyperbolic secant plus exponential distribution expressed as:

$$\rho_{\text{d}}(R, z) = \frac{M_{\text{tn}}}{4\pi h_R^2 h_z} e^{-R/h_R} \text{sech}^2(-z/h_z) \text{ M}_{\odot} \text{pc}^{-3}, \quad (10)$$

where  $R$  and  $z$  are the natural cylindrical coordinates of the axisymmetric disc,  $h_R = 2.5$  kpc is the scale length of the disc, and  $h_z = 0.352$  kpc is the scale height of the thin disc.  $M_{\text{tn}}$  is the mass of the thin disc, which is determined by the star formation rate. We adopt the position of the Sun to be  $R_{\text{sun}} = 8.5$  kpc,  $z_{\text{sun}} = 16.5$  pc (Freudenreich 1998). We neglect the age and mass dependence of the scale height. This thin-disc model is consistent with the model of Klypin et al. (2002) and Robin et al. (2003), and also in agreement with Hipparcos results and the observed rotation curve.

From the SF rate, the total mass of stars in the thin disc at age 10 Gyr is  $M_{\text{tn}} \approx 5.2 \times 10^{10} \text{ M}_{\odot}$ . Combining the thin disc model and the mass of stars in the thin disc, the stellar density in the solar neighbourhood is  $6.27 \times 10^{-2} \text{ M}_{\odot} \text{pc}^{-3}$  for the thin disc. These values are consistent with the Hipparcos result,  $(7.6 \pm 1.5) \times 10^{-2} \text{ M}_{\odot} \text{pc}^{-3}$  (Creze et al. 1998) and the dynamical structure of the thin disc (Klypin et al. 2002; Robin et al. 2003). The local density of DDs in the model is  $1.98 \times 10^{-4} \text{ pc}^{-3}$ .

**Table 2.** The contributions of different star formation stages to the numbers of DDs at present day in the quasi-exponential star formation model in the thin disc.

|                | He+He    | CO+He    | CO+CO    | ONeMg+X |
|----------------|----------|----------|----------|---------|
| 0–6 Gyr        | 48559102 | 19070461 | 51364818 | 5818348 |
| 6–8 Gyr        | 3027804  | 2401504  | 12752445 | 1522955 |
| 8–9 Gyr        | 178166   | 233402   | 5365912  | 695988  |
| 9–9.4 Gyr      | 458      | 1630     | 1347366  | 256836  |
| 9.4–9.95 Gyr   | 0        | 5        | 774012   | 309854  |
| 9.95–9.975 Gyr | 0        | 0        | 0        | 309     |
| 9.975–10 Gyr   | 0        | 0        | 0        | 0       |
| 0–10 Gyr       | 51765530 | 21707002 | 71604553 | 8604290 |

## 3 IMPACT OF STAR FORMATION ON THE DD POPULATION

The presence of unevolved DDs in Fig. 1 indicates the existence of a critical time when the first DD of each type was just born. For ONeMg+X, CO+CO, CO+He, and He+He DDs respectively, the times are 25 Myr, 50 Myr, 560 Myr, and 650 Myr. Figure 5 illustrates the contribution of different epochs of star formation to the present-day distribution of total mass and orbital periods of the DDs. We here distinguish the star formation for the current thin disc in six stages, which are (a)  $0 \leq t_{\text{sf}}/\text{Gyr} < 6$ , (b)  $6 \leq t_{\text{sf}}/\text{Gyr} < 8$ , (c)  $8 \leq t_{\text{sf}}/\text{Gyr} < 9$ , (d)  $9 \leq t_{\text{sf}}/\text{Gyr} < 9.4$ , (e)  $9.4 \leq t_{\text{sf}}/\text{Gyr} < 9.95$ , and (f)  $9.95 \leq t_{\text{sf}}/\text{Gyr} < 9.975$ , with the current disc age assumed to be 10 Gyr. We do not obtain any DD for star formation taking place after 9.975 Gyr. Figure 5 shows that the formation of very close compact binaries ( $\log f > -2.5$ ) is sensitive to star formation between 8 and 9.95 Gyr after the thin disc formed, which means that these DDs are most likely to be young. Their MS+MS progenitors formed between 50 Myr and 2000 Myr ago.

The total stellar mass formed during the time represented by each panel of Fig. 5 is 3.62, 0.85, 0.38, 0.15, 0.19, and  $0.0087 \times 10^{10} \text{ M}_{\odot}$  (a to f). The current number of DDs in the thin disc derived from each star formation epoch in the figure is given in table 2. These numbers indicate that, for current He+He and CO+He DDs, a large number (93.8% and 87.8%) have ages greater than 4 Gyr, while only 71.9% and 67.8% of CO+CO and ONeMg+X have ages in the same range. A significant number (3.1% and 6.7%) of CO+CO and ONeMg+X DDs have been produced by the last 1 Gyr of star formation. The number of He+He and CO+He DDs from this period is negligible. However, Yu & Jeffery (2011) show that DDs with ages less than 2 Gyr would contribute substantially to the amplitude of the gravitational wave signal in several frequency bands.

According to the classification of the star formation stages and the critical time for the birth of DDs, we can see from Fig. 5 that the MS+MS progenitors of CO+CO DDs are formed before  $t_{\text{sf}} \approx 9.95$  Gyr. The youngest CO+He DD has an age of about 560 Myr, but the majority of their MS progenitors formed  $>600$  Myr ago. These results are consistent with stellar evolution calculations.

Note that in the stellar evolution model a fraction of ONeMg white dwarfs become neutron stars and stellar-mass black holes due to accretion-induced collapse. These do not form type Ia supernovae and are not otherwise considered in our results.

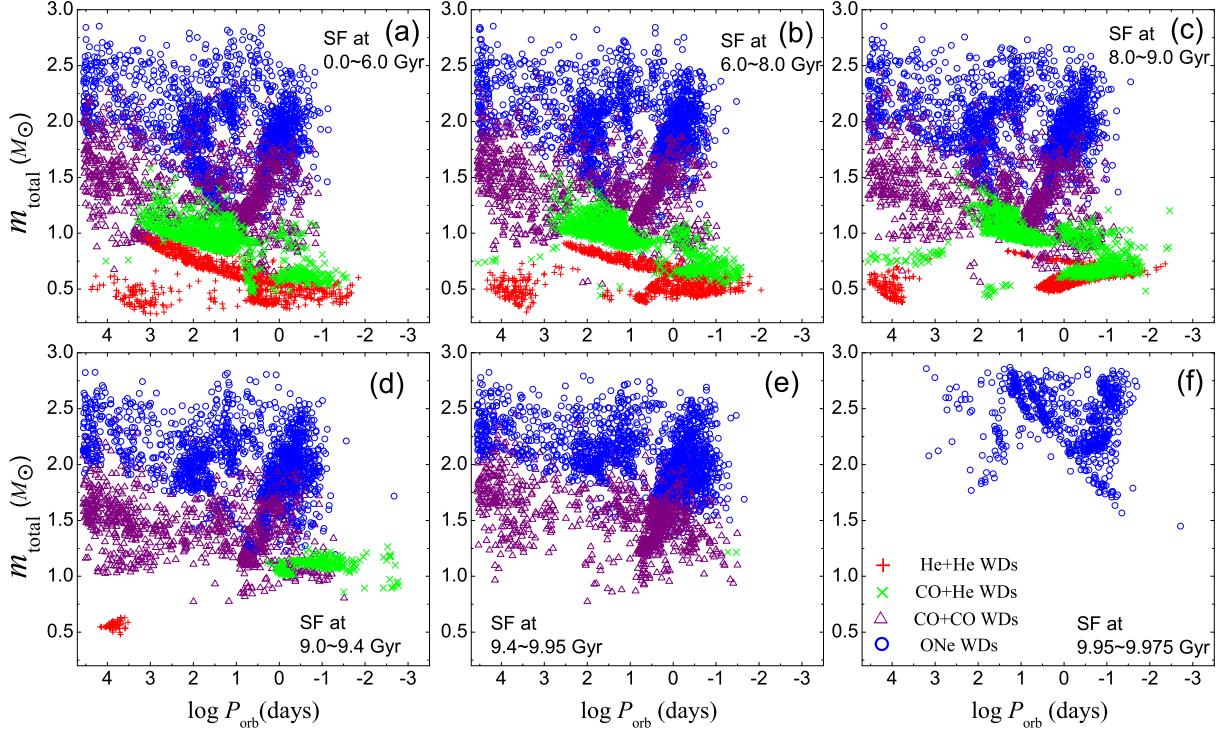


**Figure 5.** The influence of different stages of star formation on the orbital periods and the total mass (primary mass + secondary mass) of present DDs.

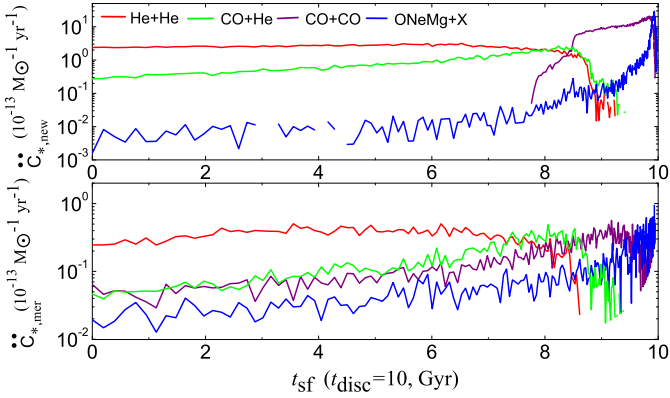


**Figure 6.** The rate contribution function of star formation epochs to the present birth rates ( $\dot{C}_{*,\text{new}}$ , top) and merger rates ( $\dot{C}_{*,\text{mer}}$ , bottom) of DDs with respect to star formation time  $t_{\text{sf}}$  in sample.

#### 4 COMPARISON OF DIFFERENT STAR FORMATION MODELS

We have simulated the present DD population with a quasi-exponential declining SF rate. In order to see the influence on the DDs from different SF models, we have arbitrarily constructed another three simple SF models and calculated the birth rates, merger rates, and the number of DDs. In addition to the quasi-exponential SF model described above, these are :

*Instantaneous SF.* A single star burst takes place only at the for-

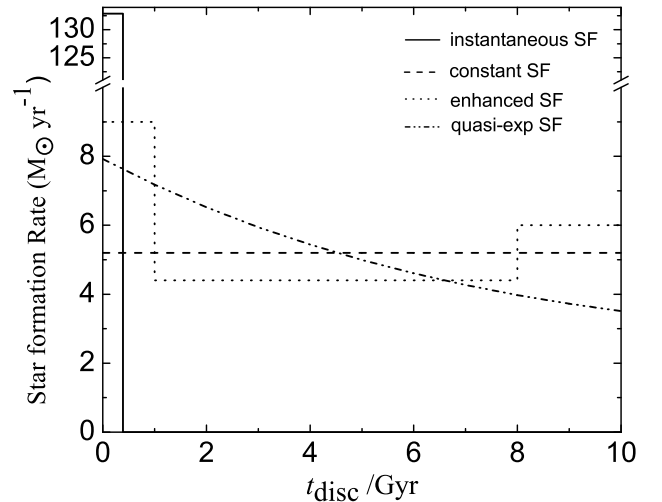


**Figure 7.** Star formation rates in star formation models.

mation of the thin disc with

$$S = \begin{cases} M_{\text{tn}}/t_0, & 0 \leq t_{\text{disc}} \leq t_0, \\ 0, & t_0 < t_{\text{disc}} \leq 10 \text{ Gyr}. \end{cases} \quad (11)$$

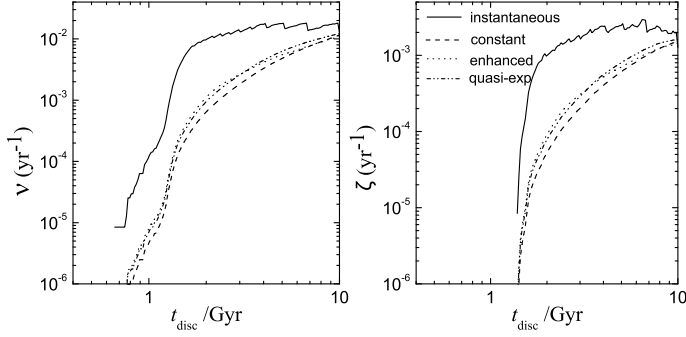


**Figure 8.** Birth rates ( $\nu$ , left) and merger rates ( $\zeta$ , right) of He+He DDs in the different star formation models.

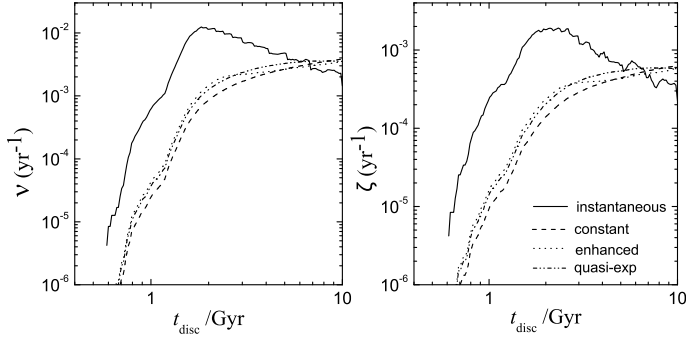


**Figure 9.** As Fig. 8 for CO+He DDs.

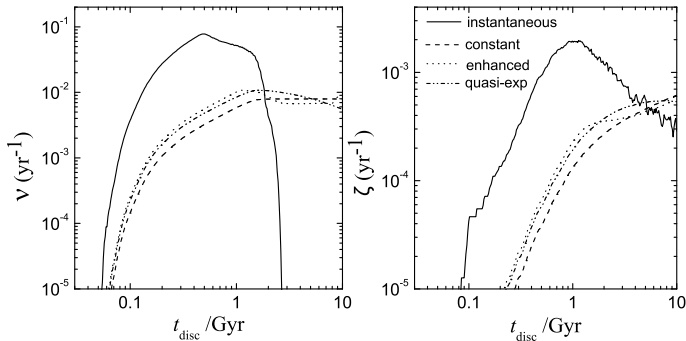


**Figure 10.** As Fig. 8 for CO+CO DDs.

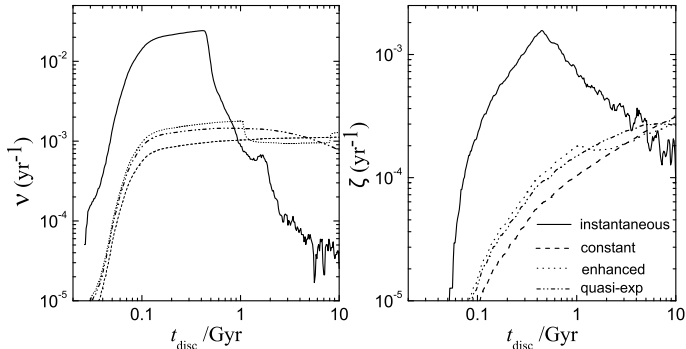


**Figure 11.** As Fig. 8 for ONeMg+X DDs.

We take  $t_0 = 391$  Myr, so the resulting SF rate in this model is  $132.9 M_{\odot} \text{ yr}^{-1}$  on average from  $t_{\text{sf}} = 0$  to 391 Myr. There is no subsequent star formation.

*Constant SF.* A constant SF rate at an average rate of

$$S = 5.2 M_{\odot} \text{ yr}^{-1}, \quad 0 \leq t_{\text{disc}} \leq 10 \text{ Gyr}. \quad (12)$$

*Enhanced SF.* An enhanced SF rate during  $t_{\text{disc}}$  from 8 to 10 Gyr,

$$S = \begin{cases} 9, & 0 \leq t_{\text{disc}} \leq 1 \text{ Gyr}, \\ 4.4, & 1 < t_{\text{disc}} \leq 8 \text{ Gyr}, \\ 6, & 8 < t_{\text{disc}} \leq 10 \text{ Gyr}. \end{cases} \quad (13)$$

Each model produces a present stellar mass of  $5.2 \times 10^{10} M_{\odot}$  in the thin disc with present age  $t_{\text{disc}} = 10$  Gyr in agreement with the dynamic mass of the thin disc (Klypin et al. 2002).

Figures 6 and 7 show the star-formation contribution function  $\dot{C}_*$  in our sample to the birth rates and merger rates of the DDs and the SF rate for each SF model. These two variables are needed to calculate the birth rates and merger rates in the thin disc in Eq. 7. The many small oscillations on the star-formation contribution functions in Fig. 6 (and Fig. 2) are due to the statistical noise of the Monte Carlo simulations.

Figures 8 to 11 show the birth rates ( $\nu$ ) and merger rates ( $\zeta$ ) of the four types of DD in the four models. We see that the instantaneous SF differs greatly from the other three models. As a result of the impact of a high SF rate at the formation of the thin disc,  $\nu$  and  $\zeta$  in the instantaneous SF model increase very sharply to reach a maximum value several times greater than in all other models.  $\nu$  and  $\zeta$  subsequently decrease slowly for the He+He DDs since they have a long  $t_{\text{MS}}$ . In the cases of the other three types of DD in the instantaneous SF model, the decline of  $\nu$  and  $\zeta$  is faster than He+He DDs due to the shorter  $t_{\text{MS}}$ . When  $t_{\text{disc}} > 2.3$  Gyr, roughly the longest  $t_{\text{MS}}$  of CO+CO DD, there are no more new-born CO+CO DDs. ONeMg+X DDs show a reduction in  $\nu$  and  $\zeta$ , except for the ONeMg+He DDs which make a residual contribution to  $\nu$  as the disc continue to evolve. Again, some oscillations are seen in the birth and merger rates in the instantaneous SF model. These are due to statistical noise from the contribution functions produced by the Monte Carlo simulations, and numerical noise from the quadrature of Eq. 7.

A big difference for  $\nu$  and  $\zeta$  in the other three models can also be seen from the figures. Enhanced SF causes the present  $\nu$  and  $\zeta$  of CO+CO and ONeMg+X DDs to be slightly higher than constant SF, while the quasi-exponential SF can produce a higher  $\nu$  and  $\zeta$  of CO+CO and ONeMg+X DDs than enhanced SF when  $t_{\text{disc}} < 4$  Gyr. When  $t_{\text{disc}} > 4$  Gyr, we find  $\nu$  and  $\zeta$  of CO+CO and ONeMg+X DDs decrease dramatically in the quasi-exponential SF model, while the values of  $\nu$  and  $\zeta$  in the constant SF model remain almost constant and higher than the  $\nu$  and  $\zeta$  in the quasi-exponential SF model, up to  $t_{\text{disc}} = 10$  Gyr. The significant decreases and increases of the values of  $\nu$  and  $\zeta$  of CO+CO and ONeMg+X DDs in the enhanced SF model are the response of these variables to sudden changes in the SF rate. The present values of  $\nu$  and  $\zeta$  are similar because we adopt a similar value of the average SF rate at the present age of the thin disc in these three models.

The present number and the total merger number of different types of DDs are shown in Figs. 12 to 15. A similar evolutionary history of the numbers for various types of DD is generated by the continuous SF models since the average values of the SF rate are similar in these SF models. The instantaneous SF model produces

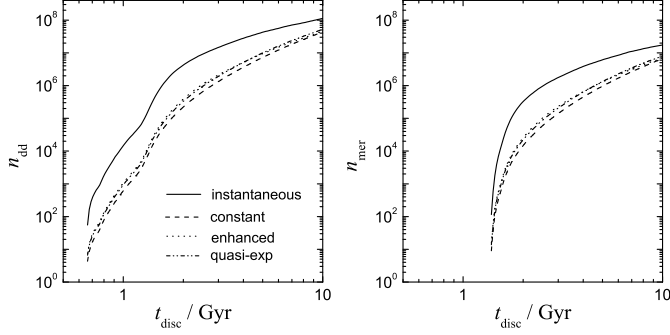


**Figure 12.** Present number ( $n_{\text{dd}}$ , left) and total merger number ( $n_{\text{mer}}$ , right) of He+He DDs in the different star formation models.

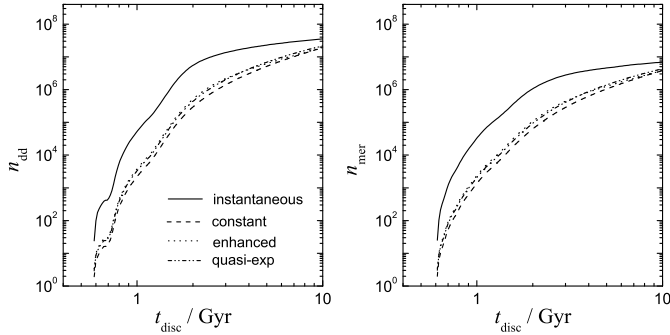


**Figure 13.** As Fig. 12 for CO+He DDs.

a slightly higher present numbers of DDs than the other three SF models, and has a distinctly different evolution.

A delay time, which represents the time from when the first DD was born to when the first DD merged, can certainly be found in each model if we compare the left panel and the right panel in each figure. The delay time can not be less than the shortest life time  $t_{\text{DD}}$  of a DD, and is affected significantly by stellar evolution models and population synthesis parameters (*e.g.* the IMF). Since we use the same stellar evolution model and population synthesis parameters for each single epoch of the SF in our simulations, the delay time is a constant for each SF model. We list the delay time for different types of DD in Table 6.

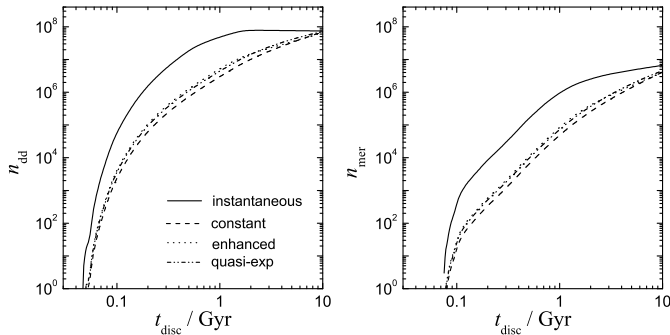


**Figure 14.** As Fig. 12 for CO+CO DDs.

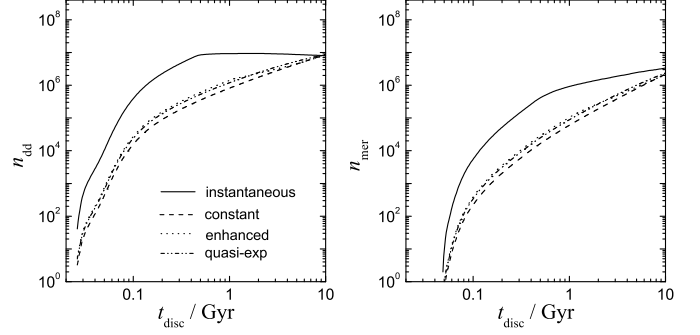


**Figure 15.** As Fig. 12 for ONeMg+X DDs.

**Table 3.** As table 2 except for the instantaneous star formation model.

|              | He+He     | CO+He    | CO+CO    | ONeMg+X |
|--------------|-----------|----------|----------|---------|
| 0–0.391 Gyr  | 112790783 | 35296981 | 74199554 | 7979607 |
| 0.391–10 Gyr | 0         | 0        | 0        | 0       |
| 0–10 Gyr     | 112790783 | 35296981 | 74199554 | 7979607 |

## 5 SUPERNOVAE

We have been concerned about the details of birth rate and number of DDs in the present simulation. However, we suggest that Eq. 7 (to calculate the birth rate) and Eq. 6 and 8 (to calculate the number) are valid for almost any type of star. The only thing required is to determine the corresponding contribution of each SF epoch to the numbers of the stars in question with respect to the variation of the SF (*i.e.*  $t_{\text{sf}}$ ). In terms of the determination of the contribution, it is important to determine all possible formation channels. Otherwise we should specify that the birth rate or number correspond to a specific formation channel. We would like to take two important examples, type Ia supernovae (SNIa) and core collapse supernovae (ccSN, including type Ib/Ic and type II).

Previous studies (*e.g.* Iben & Tutukov (1984); Tutukov et al. (1992); Iben & Tutukov (1997); Yungelson & Livio (1998, 2000); Dahlen et al. (2004)) indicate that mergers of DDs with a total mass exceeding the Chandrasekhar mass limit ( $M_{\text{ch}}$ ) would be one formation channel to produce SNIa. We here investigate the birth rate of SNIa from the mergers of DDs, and we constrain the progenitors to be those DDs with total mass  $> M_{\text{ch}} = 1.38 M_{\odot}$  which can merge in the time  $t_{\text{disc}}$  to  $t_{\text{disc}} + \delta t_{\text{disc}}$ .

**Table 4.** As table 2 except for the constant star formation model.

|                | He+He    | CO+He    | CO+CO    | ONeMg+X |
|----------------|----------|----------|----------|---------|
| 0–6 Gyr        | 39518987 | 15920357 | 43845056 | 4979173 |
| 6–8 Gyr        | 2484043  | 2889597  | 15507241 | 1852669 |
| 8–9 Gyr        | 1370423  | 312505   | 7286013  | 946315  |
| 9–9.4 Gyr      | 649      | 2309     | 1918541  | 366020  |
| 9.4–9.95 Gyr   | 0        | 8        | 1129931  | 454258  |
| 9.95–9.975 Gyr | 0        | 0        | 1        | 462     |
| 9.975–10 Gyr   | 0        | 0        | 0        | 0       |
| 0–10 Gyr       | 43374102 | 19124776 | 69686783 | 8598897 |

**Table 5.** As table 2 except for the enhanced star formation model.

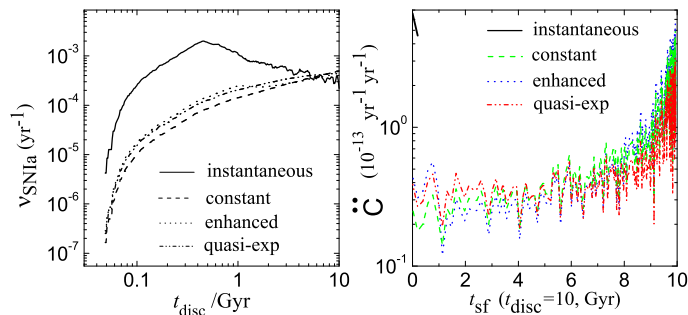
|                | He+He    | CO+He    | CO+CO    | ONeMg+X |
|----------------|----------|----------|----------|---------|
| 0–6 Gyr        | 42952616 | 16651902 | 44547319 | 5041578 |
| 6–8 Gyr        | 3094596  | 2472828  | 13270620 | 1585457 |
| 8–9 Gyr        | 267637   | 351727   | 8315871  | 1080840 |
| 9–9.4 Gyr      | 748      | 2666     | 2213701  | 422330  |
| 9.4–9.95 Gyr   | 0        | 7        | 1303767  | 524144  |
| 9.95–9.975 Gyr | 0        | 0        | 1        | 533     |
| 9.975–10 Gyr   | 0        | 0        | 0        | 0       |
| 0–10 Gyr       | 46315597 | 19479130 | 69651279 | 8654882 |

**Table 6.** The delay time, which is from the time the first DD was born to the time the first merged DD appears, for each type of DD.

|                  | He+He  | CO+He | CO+CO | ONeMg+X |
|------------------|--------|-------|-------|---------|
| delay time (Myr) | 724.03 | 23.94 | 28.65 | 22.39   |

The birth rates of SNIa for the four SF models are shown in the left panel in Fig. 16, and the rate contribution function from each single epoch in the four models is shown in the right panel in the same figure. The calculation of the rate contribution function is from the number of DDs satisfying the conditions to become SNIa in our simulation. Note that the curve in the right panel is also the age distribution of SNIa, taking into account the SF rate in the thin disc. This figure indicates that both old and young DDs contribute to the present SNIa rates.

From the left panel, we see that the birth rate of SNIa from the instantaneous SF model reaches its maximum value very quickly with the evolution of the thin disc. The maximum value is significantly higher than that in another three SF models since the initial SF rate in the instantaneous SF model is more than  $\sim 30$  times that in other SF models. The enhanced SF model produces the highest present rate of SNIa in the four SF models. This is because the present SF contributes the majority of mergers. Again, from Fig. 16, continuous SF is also the reason why the rate of SNIa keeps growing with the evolution of the thin disc. The present-day SNIa rate is about 2.19, 4.92, 5.07, and  $4.34 \times 10^{-4} \text{ yr}^{-1}$  for the in-


**Figure 16.** The rates of type Ia supernovae from double degenerate mergers channel in different star formation models (left panel), and the rate contribution function to the present-day ( $t_{\text{disc}} = 10 \text{ Gyr}$ ) supernovae rates in the thin disc (right panel).

stantaneous, constant, enhanced, and quasi-exponential SF models respectively.

We have to emphasize that we here only take into account the merger channel for the rate of thin-disc SNIa. This leads to our results being less than the occurrence rate inferred from observations,  $\sim 4 \times 10^{-3} \text{ yr}^{-1}$  (Cappellaro et al. 1997), as a few other formation channels would contribute to the observed occurrence rate (Yungelson & Livio 2000; Han & Podsiadlowski 2004; Hachisu et al. 2008).

We note that the occurrence (or birth) rate of SNIa at  $t_{\text{disc}} = 10 \text{ Gyr}$  in our simulations is smaller than in some other recent theoretical studies (e.g. Ruiter et al. (2009); Mennekens et al. (2010)) by a factor of 1.5–4. Since all these studies (including ours) adopt the same IMF for the primary main sequence stars, the same flat distribution for initial mass ratio, and the same initial eccentricity distribution, we infer that the differences between our study and others are mainly caused by the initial distribution of orbital separations and by the treatment of mass transfer and mass loss during binary evolution.

Both Ruiter et al. (2009) and Mennekens et al. (2010) adopt a distribution of the orbital separation  $\frac{dn}{da} \propto a^{-1}$  (Abt 1983) when  $a \leq 10^5 R_{\odot}$ , while we use a distribution of  $\propto a^{0.2}$  (Griffin 1985; Han 1998) for  $a \leq 10 R_{\odot}$ , and  $\propto a^{-1}$  for  $10 \leq a \leq 5.75 \times 10^6 R_{\odot}$ . This may lead to the generation of more close DDs in their models than our model.

For common-envelope ejection, we adopt the  $\gamma$ -algorithm (Nelemans & Tout 2005) and fix  $\gamma = 1.5$ . Other studies use the  $\alpha$ -algorithm (Webbink 1984). Increasing the common-envelope ejection efficiency (for example, increasing  $\alpha\lambda = 0.5 \rightarrow 1.0$ ) results in more binaries going through a double common-envelope phase to become close DDs, and hence forming potential SNIa progenitors. A close comparison between the studies implies that the common-envelope ejection efficiency is lower in our calculation than in others. In the most extreme case, the Yungelson (2010) SNIa birth rate from the DD merger channel is higher than ours by a factor of  $\sim 10$  because they adopted a very high common-envelope ejection efficiency ( $\alpha\lambda = 2.0$ ) and a higher SF rate ( $\sim 8 M_{\odot} \text{ yr}^{-1}$ ).

A significant difference between the studies concerns the star-formation history for early-type (elliptical) galaxies. Both Ruiter et al. (2009) and Mennekens et al. (2010) approximate “instantaneous star formation” by a  $\delta$ -function star-burst. Our approximation of “instantaneous SF” assumes that the initial star-burst lasted a few million years at a constant rate. This leads to the peak value of the SNIa rate occurring rather later in our models than in the studies in Ruiter et al. (2009) and Mennekens et al. (2010). However, none of these approximations may reflect the true SF history of early-type galaxies; recent studies indicate that bright early-type galaxies show signs of current star formation (Yi et al. 2005) and, by inference, may have experienced intermittent star-burst episodes.

The case of ccSN is easier than that of SNIa. Their progenitors, main sequence stars with mass approximately greater than  $8 M_{\odot}$ , evolve very quickly on a timescale  $\lesssim 20 \text{ Myr}$ . This is even shorter than the  $t_{\text{MS}}$  of ONeMg+X (see Fig. 1), so all the newborn ccSN results from SF after a few tens Myr (see criterion in §2.3). Then the SF rate can be regarded as a constant  $S(t_{\text{disc}})$ . From Eq. 7, we have the birth rate of the supernovae  $SNR(t_{\text{disc}}) \approx [N_{\text{ccSN}}/m_{\text{total}}] \cdot S(t_{\text{disc}})$ , where  $N_{\text{ccSN}}$  is the number of stars going supernova in a calculation of a sample of main sequence stars,  $m_{\text{total}}$  represents the total mass of the sample, and  $t_{\text{disc}} = 10 \text{ Gyr}$ . Using the same parameters as in the simulation in this paper, we obtain  $N_{\text{ccSN}}/m_{\text{total}} \approx 4.5 \times 10^{-3} M_{\odot}^{-1}$  and so  $SNR(10) \approx$

2.34, 2.7 and 1.58 century<sup>-1</sup> for the three continuous SF models. These values are consistent with the observations of 1.2 – 3 century<sup>-1</sup> (Smith et al. 1978; van den Bergh & McClure 1994; McKee & Williams 1997; Timmes et al. 1997; Diehl et al. 2006) in terms of the mass of <sup>26</sup>Al, the number of massive stars in the localized HII region and the extragalactic supernova scaled calculation.

## 6 DISCUSSION

Our simulation is based only on theory with some simple assumptions. The final outputs, the rates and numbers, are derived from two key inputs which are the SF rate and the contribution functions for the evolved stars. On the other hand, if we know the rates and numbers of objects in a galaxy, especially some types of exotic stars, we are able to do a deconvolution by setting the observed rate as an input parameter to derive the SF rate at specific epochs. In fact, this method is used to obtain the current SF rate via the observation of supernovae (Heger et al. 2003; Diehl et al. 2006) and a global SF rate by observations of late type main sequence stars (Rocha-Pinto et al. 2000). The contribution functions provide an important link between SF history and the diverse stellar components in different galaxies, since they reflect the sensitivity of a group of the same type of stars to the SF history of a galaxy.

The time grid  $\delta t_{\text{sf}}$  (or  $\delta t_{\text{disc}}$ ) can cause some uncertainties. For the quasi-exponential declining SF rate, another computation with a low-resolution time grid of  $\delta t_{\text{sf}} = 0.026$  results in positive deviations from the high resolution time grid ( $\delta t_{\text{sf}} = 0.00867$ ) of 1.03%, 0.82%, 0.04% and 0.21% for the birth rates of He+He, CO+He, CO+CO and ONeMg+X DDs respectively; the deviations of the numbers are 3.97%, 2.53%, 1.13% and 0.87% for the different types of DDs. In the new grid, the deviations of the numbers calculated from Eq. 6 compared with Eq. 8 are 4.7%, 2.8%, 1.5% and 1.4% for each type of DD. The time error for different stellar evolution phase in our simulation is less than 4.2%.

## 7 CONCLUSION

In this paper we have investigated the relation between the evolution of birth rates, merger rates and numbers of different types of DD and the SF history in the thin disc of the Milky Way Galaxy. By analysing how a quasi-exponentially declining SF rate influences the rates and observed numbers of DDs with respect to the evolution of the disc and SF, we find that SF between 0 and  $\sim 8$  Gyr dominates the present rates and total numbers of He+He DDs and CO+He DDs. Similarly, the current numbers of CO+CO and ONeMg+X DDs mainly come from early SF, although the later SF (e.g. 4 to 8 Gy) contributes more CO+CO than it does for He+He which are the two largest DD population in the thin disc.

However, the present birth and merger rates of CO+CO and ONeMg+X DDs are strongly governed by the recent star formation (i.e. 8 to 9.95 Gyr). SF before  $\approx 7.5$  Gyr does *not* contribute to the present birth rates of CO+CO and ONeMg+X DDs, but it has some contribution to the merger rates. More importantly, with the SF history related population synthesis approach in this paper, not only are we able to determine the rates and numbers of DDs, but we can also obtain the distributions of properties of current DD population from different stages of SF.

We have compared the impact of different SF models, namely the instantaneous, the constant, the enhanced, and the quasi-exponential SF, on the rates and numbers of DDs and the rates of

two types of supernovae. The evolution tracks of the rates and numbers from the four models are quite different. A distinct difference can be found between the instantaneous model and the other three continuous SF models. This model gives historical rates and numbers obviously higher than the other three models. However, the present rates of DDs from this model are apparently lower than the other three models.

In addition to the DDs, we have calculated the rates of SNIa and ccSN. The evolution of the rates of SNIa is basically similar in the four SF models, but the instantaneous model can produce a higher rate in the past because of the very high SF rate at the formation of the thin disc. The present rates of SNIa are 2.19, 4.92, 5.07, and  $4.34 \times 10^{-4}$  yr<sup>-1</sup> for the instantaneous, the constant, the enhanced, and the quasi-exponential SF models respectively. The rates of ccSN from all four SF models,  $\approx 1.5$  to 3 century<sup>-1</sup>, are consistent with the observations.

## ACKNOWLEDGMENTS

The Armagh Observatory is supported by a grant from the Northern Ireland Dept. of Culture Arts and Leisure. The authors are grateful to Prof. Lev Yungelson for useful suggestions, and to colleagues at the Armagh Observatory for their stimulating discussion. We thank the referee for the useful suggestions and comments.

## REFERENCES

- Abt H. A., 1983, ARA&A, 21, 343
- Cappellaro E., Turatto M., Tsvetkov D. Y., Bartunov O. S., Pollas C., Evans R., Hamuy M., 1997, A&A, 322, 431
- Creze M., Chereul E., Bienayme O., Pichon C., 1998, A&A, 329, 920
- Cropper M., Harrop-Allin M. K., Mason K. O., Mittaz J. P. D., Potter S. B., Ramsay G., 1998, MNRAS, 293, L57
- Dahlen T., Strolger L., Riess A. G., Mobasher B., Chary R., Conselice C. J., Ferguson H. C., Fruchter A. S., Gialalisco M., Livio M., Madau P., Panagia N., Tonry J. L., 2004, ApJ, 613, 189
- Diehl R., Halloin H., Kretschmer K., Lichti G. G., Schönfelder V., Strong A. W., von Kienlin A., Wang W., Jean P., Knödseder J., Roques J., Weidenspointner G., Schanne S., Hartmann D. H., Winkler C., Wunderer C., 2006, Nature, 439, 45
- Evans C. R., Iben I. J., Smarr L., 1987, ApJ, 323, 129
- Farmer A., Roelofs G., 2010, ArXiv e-prints
- Freudenreich H. T., 1998, ApJ, 492, 495
- Gokhale V., Peng X. M., Frank J., 2007, ApJ, 655, 1010
- Griffin R. F., 1985, in P. P. Eggleton & J. E. Pringle ed., NATO ASIC Proc. 150: Interacting Binaries The distributions of periods and amplitudes of late-type spectroscopic binaries. pp 1–12
- Hachisu I., Kato M., Nomoto K., 2008, ApJ, 683, L127
- Han Z., 1998, MNRAS, 296, 1019
- Han Z., Podsiadlowski P., 2004, MNRAS, 350, 1301
- Heger A., Fryer C. L., Woosley S. E., Langer N., Hartmann D. H., 2003, ApJ, 591, 288
- Hurley J. R., Pols O. R., Tout C. A., 2000, MNRAS, 315, 543
- Hurley J. R., Tout C. A., Pols O. R., 2002, MNRAS, 329, 897
- Iben Jr. I., Tutukov A. V., 1984, ApJ, 54, 335
- Iben Jr. I., Tutukov A. V., 1997, ApJ, 491, 303
- Klypin A., Zhao H., Somerville R. S., 2002, ApJ, 573, 597
- Kroupa P., Tout C. A., Gilmore G., 1993, MNRAS, 262, 545
- Majewski S. R., 1993, ARA&A, 31, 575

- Marsh T. R., Nelemans G., Steeghs D., 2004, MNRAS, 350, 113  
McKee C. F., 1989, ApJ, 345, 782  
McKee C. F., Williams J. P., 1997, ApJ, 476, 144  
Mennekens N., Vanbeveren D., De Greve J. P., De Donder E., 2010, A&A, 515, A89+  
Nelemans G., Tout C. A., 2005, MNRAS, 356, 753  
Nelemans G., Yungelson L. R., Portegies Zwart S. F., 2001, A&A, 375, 890  
Nelemans G., Yungelson L. R., Portegies Zwart S. F., 2004, MNRAS, 349, 181  
Phleps S., Meisenheimer K., Fuchs B., Wolf C., 2000, A&A, 356, 108  
Popper D. M., 1980, ARA&A, 18, 115  
Ramsay G., Hakala P., Wu K., Cropper M., Mason K. O., Córdoba F. A., Priedhorsky W., 2005, MNRAS, 357, 49  
Robin A. C., Reylé C., Derrière S., Picaud S., 2003, A&A, 409, 523  
Rocha-Pinto H. J., Scalo J., Maciel W. J., Flynn C., 2000, A&A, 358, 869  
Ruiter A. J., Belczynski K., Benacquista M., Larson S. L., Williams G., 2010, ApJ, 717, 1006  
Ruiter A. J., Belczynski K., Fryer C., 2009, ApJ, 699, 2026  
Sackett P. D., 1997, ApJ, 483, 103  
Smith L. F., Biermann P., Mezger P. G., 1978, A&A, 66, 65  
Timmes F. X., Diehl R., Hartmann D. H., 1997, ApJ, 479, 760  
Tutukov A. V., Yungelson L. R., Iben Jr. I., 1992, ApJ, 386, 197  
van den Bergh S., McClure R. D., 1994, ApJ, 425, 205  
Webbink R. F., 1984, ApJ, 277, 355  
Wielen R., Jahrei H., Krger R., 1983, in A. G. D. Philip & A. R. Upgren ed., IAU Colloq. 76: Nearby Stars and the Stellar Luminosity Function The Determination of the Luminosity Function of Nearby Stars. pp 163–170  
Yi S. K., Yoon S.-J., Kaviraj S. e. a., 2005, ApJ, 619, L111  
Yu S., Jeffery C. S., 2010, A&A, 521, A85+  
Yu S., Jeffery C. S., 2011, Submitted  
Yungelson L., Livio M., 1998, ApJ, 497, 168  
Yungelson L. R., 2010, Astronomy Letters, 36, 780  
Yungelson L. R., Livio M., 2000, ApJ, 528, 108